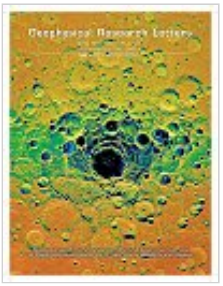

Volume 39, Issue 9

May 2012

Brief **Detailed**

Atmospheric Science

Tropical cyclone track forecasts using JMA model with ECMWF and JMA initial conditions

Munehiko Yamaguchi, Tetsuo Nakazawa, Kazumasa Aonashi

First Published: 4 May 2012 Vol: 39, L09801 | DOI: 10.1029/2012GL051473

KEY POINTS

- Error sources of typhoon track predictions are separated using the YOTC dataset
- ECMWF initial conditions reduce the prediction errors of JMA by about 10 %
- Major operational NWP centers have a northward bias in the track prediction

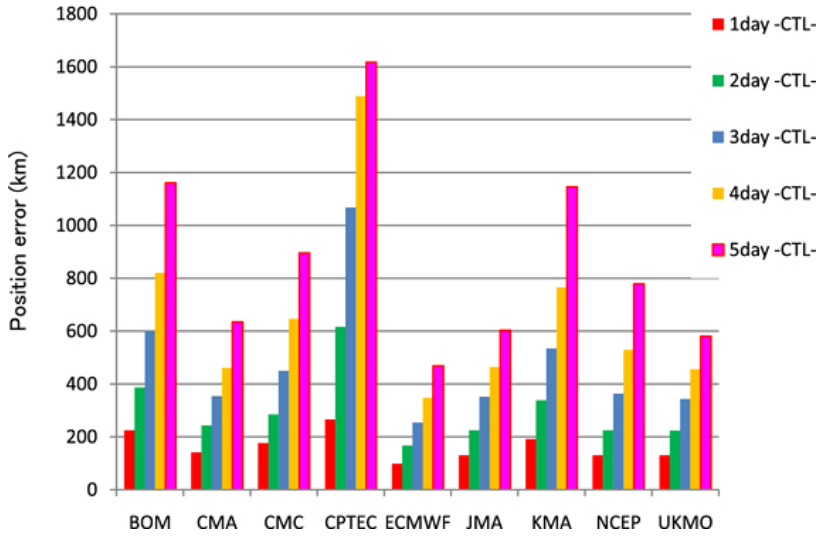

1 of 4

Direct and semi-direct radiative effects of absorbing aerosols in Europe: Results from a regional model

J. Meier, I. Tegen, B. Heinold, R. Wolke

First Published: 5 May 2012 Vol: 39, L09802 | DOI: 10.1029/2012GL050994

KEY POINTS

- Simulation of European aerosol for two time periods
- Computing direct and semi-direct radiative effects

- Semi-direct radiative effect can be considerable

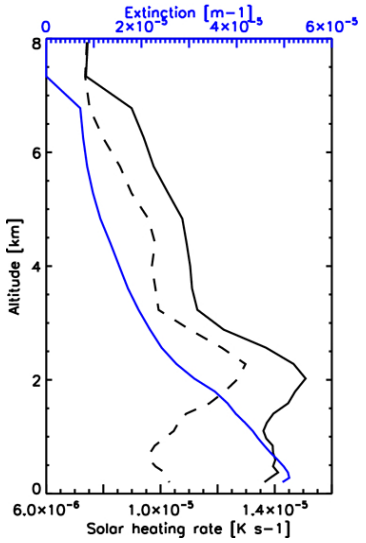

1 of 3

Reactive greenhouse gas scenarios: Systematic exploration of uncertainties and the role of atmospheric chemistry

Michael J. Prather, Christopher D. Holmes, Juno Hsu

First Published: 8 May 2012 Vol: 39, L09803 | DOI: 10.1029/2012GL051440

KEY POINTS

- A new method proposed for projecting non-CO2 GHG with uncertainty
- Enables the community to evaluate the importance of different processes
- Independent evaluation of natural and anthropogenic GHG emissions

Open Access

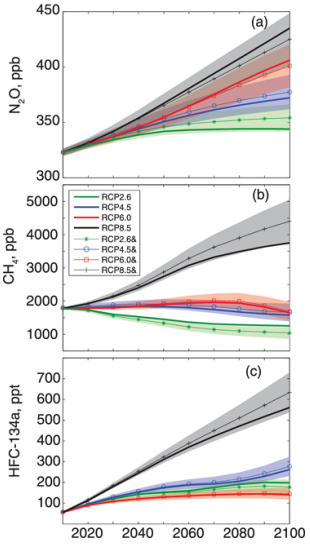

1 of 1

Strong radiative heating due to wintertime black carbon aerosols in the Brahmaputra River Valley

Rajan K. Chakrabarty, Mark A. Garro, Eric M. Wilcox, Hans Moosmüller

First Published: 9 May 2012 Vol: 39, L09804 | DOI: 10.1029/2012GL051148

KEY POINTS

- Winter-time black carbon (BC) levels one of the highest in the world
- Lower atmosphere heating rate of ~2 K/d due to BC aerosols
- Emphasizes the influence of BC emission on the extreme regional climate change

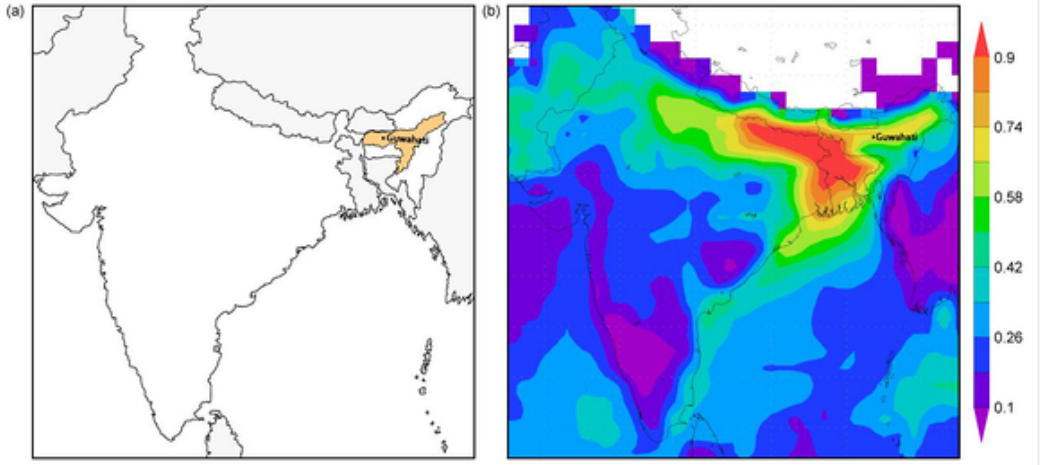

1 of 3

New particle formation and growth in biomass burning plumes: An important source of cloud condensation nuclei

Christopher J. Hennigan, Daniel M. Westervelt, Ilona Riipinen, Gabriella J. Engelhart, Taehyoung Lee, Jeffrey L. Collett Jr., Spyros N. Pandis, Peter J. Adams, Allen L. Robinson

First Published: 9 May 2012 Vol: 39, L09805 | DOI: 10.1029/2012GL050930

KEY POINTS

- New particle formation and growth occur in biomass burning plumes
- This impacts the global CCN budget, but has not been accounted for in models
- This has important implications for climate as well

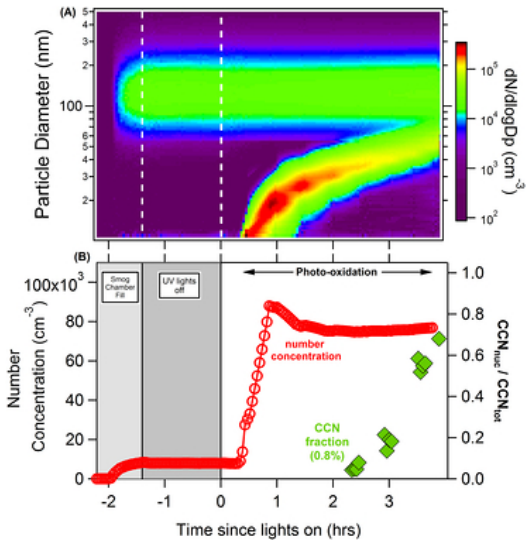

1 of 3

Potential aerosol indirect effects on atmospheric circulation and radiative forcing through deep convection

Jiwen Fan, Daniel Rosenfeld, Yanni Ding, L. Ruby Leung, Zhanqing Li

First Published: 10 May 2012 Vol: 39, L09806 | DOI: 10.1029/2012GL051851

KEY POINTS

- Aerosol invigoration (AIV) on deep convective clouds incurs positive radiative forcing
- AIV also leads to enhanced regional convergence, and a strong thermodynamic forcing
- Wind shear and cloud base T determine significance of aerosol invigoration effect

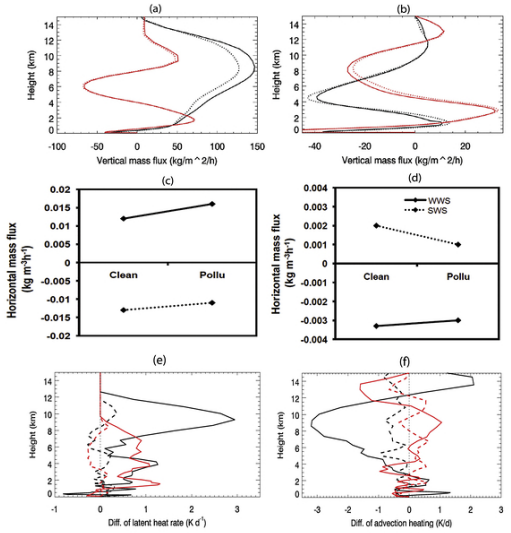

1 of 3

Geometrical and electrical characteristics of the initial stage in Florida triggered lightning

J. D. Hill, J. Pilkey, M. A. Uman, D. M. Jordan, W. Rison, P. R. Krehbiel

First Published: 11 May 2012 Vol: 39, L09807 | DOI: 10.1029/2012GL051932

KEY POINTS

- First Lightning Mapping Array VHF images of Florida triggered lightning
- Primary negative charge source for FL triggered lightning may be at 3-6 km
- VHF sources obtained from positive impulsive currents less than 10 A

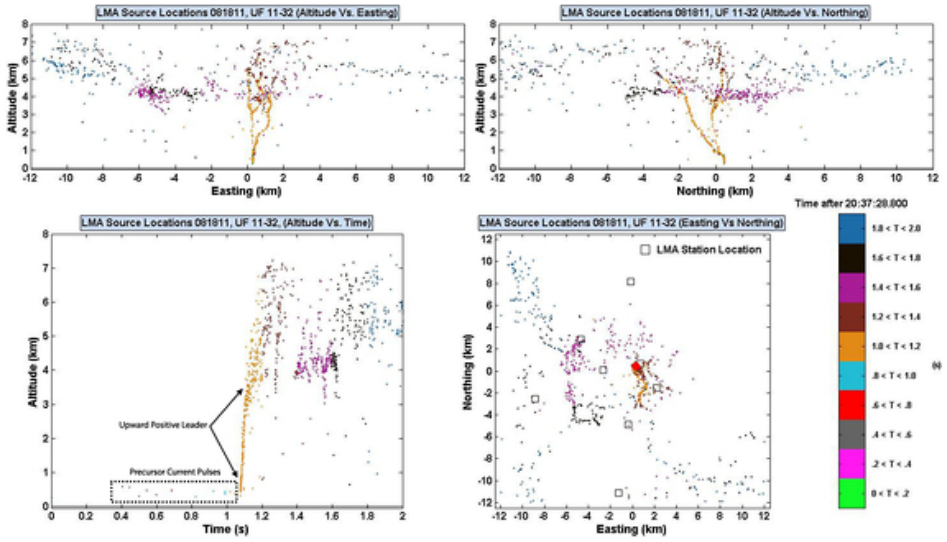

1 of 4

Effect of spectral-dependent surface albedo on Saharan dust direct radiative forcing

Xiaoyan Ma, Fangqun Yu

First Published: 12 May 2012 Vol: 39, L09808 | DOI: 10.1029/2012GL051360

KEY POINTS

- Spectral-dependent surface albedo is important on dust radiative forcing
- Employing only visible-band surface albedo in the studies may not be appropriate

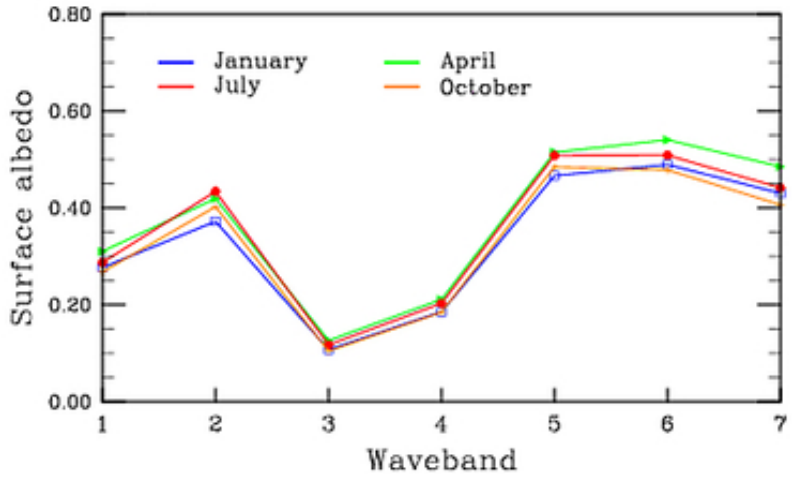

1 of 4

Increases in aerosol concentrations over eastern China due to the decadal-scale weakening of the East Asian summer monsoon

Jianlei Zhu, Hong Liao, Jianping Li

First Published: 15 May 2012 Vol: 39, L09809 | DOI: 10.1029/2012GL051428

KEY POINTS

- The weakening of the East Asian summer monsoon increases aerosol in China
- Monsoon circulation is the dominant factor that explains the increase in aerosol
- Climate change increases aerosol concentrations in China

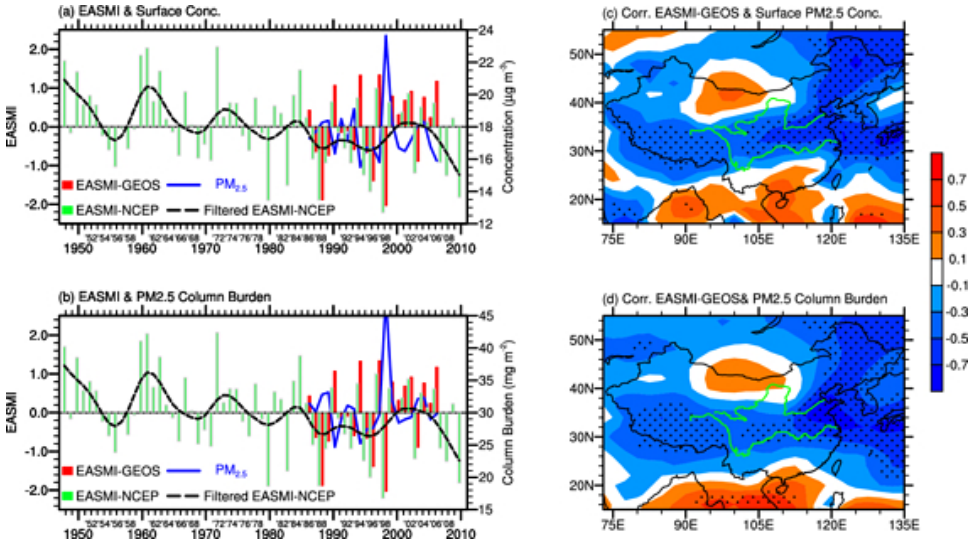

1 of 3

Climate

Climate models produce skillful predictions of Indian summer monsoon rainfall

Timothy DelSole, Jagadish Shukla

First Published: 1 May 2012 Vol: 39, L09703 | DOI: 10.1029/2012GL051279

KEY POINTS

- AOGCMs can predict Indian monsoon rainfall with skill
- Statistical models have no skill in predicting monsoon rainfall during 1960-2005
- Even ENSO-indices from AOGCMs can be used to make skill monsoon predictions

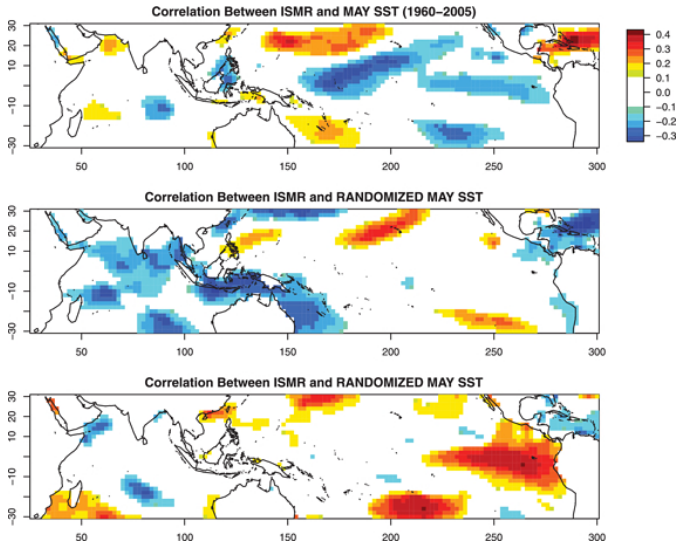

1 of 7

Late Miocene upward and outward growth of eastern Tibet and decreasing monsoon rainfall over the northwestern Indian subcontinent since ~10 Ma

Peter Molnar, Balaji Rajagopalan

First Published: 1 May 2012 Vol: 39, L09702 | DOI: 10.1029/2012GL051305

KEY POINTS

- The growth of Tibet has affected south Indian climate on geological time scales
- The effect is not a strengthened, but a weakened monsoon
- We must understand the monsoon as being more than All-India-Rainfall

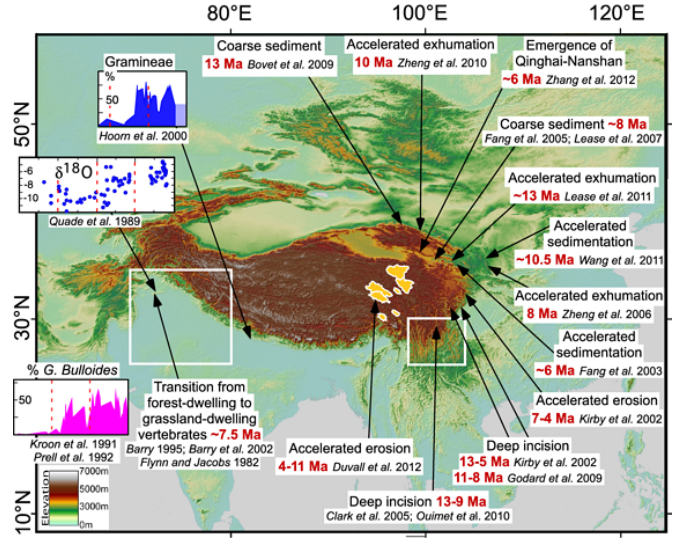

1 of 3

Recent weakening of northern East Asian summer monsoon: A possible response to global warming

Congwen Zhu, Bin Wang, Weihong Qian, Bo Zhang

First Published: 1 May 2012 Vol: 39, L09701 | DOI: 10.1029/2012GL051155

KEY POINTS

- The warming surface air temperature near Lake Baikal (LB) caused a weak EASM
- The warming near LB maintains an anomalous anticyclone and northeasterlies in EA
- The global warming is likely responsible for the recent weakening of EASM

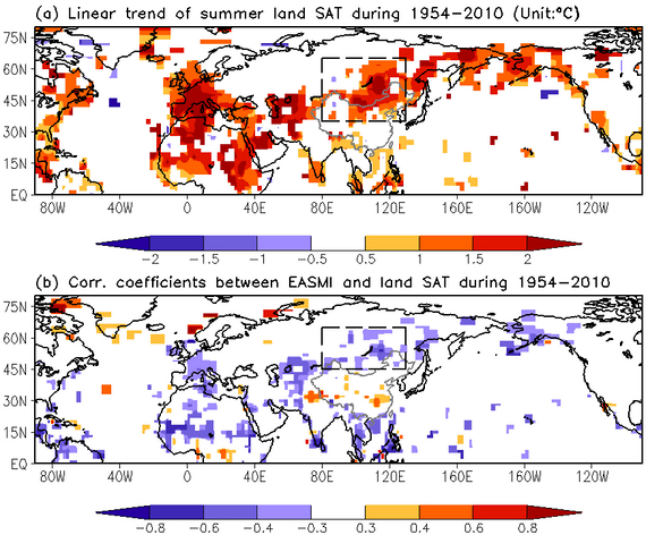

1 of 5

The role of summer surface wind anomalies in the summer Arctic sea ice extent in 2010 and 2011

Masayo Ogi, John M. Wallace

First Published: 2 May 2012 Vol: 39, L09704 | DOI: 10.1029/2012GL051330

KEY POINTS

- Arctic sea ice in 2010 and 2011 was controlled by summer surface wind forcing
- Summer atmospheric conditions determine the amount of summer Arctic sea ice
- Anticyclonic wind anomalies play an important role in the retreat of sea ice

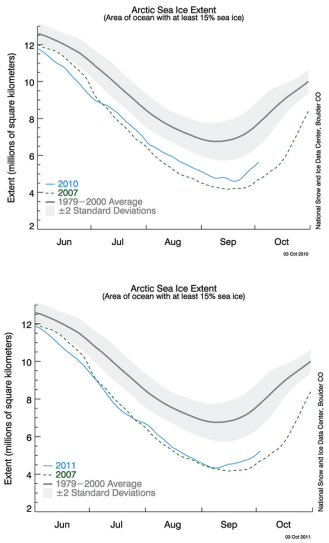

1 of 5

A 21st century shift in the relationship between ENSO SST and warm water volume anomalies

Michael J. McPhaden

First Published: 3 May 2012 Vol: 39, L09706 | DOI: 10.1029/2012GL051826

KEY POINTS

- The relationship between ENSO SST and upper ocean heat content is changing
- These changes are related to the increase in central Pacific El Ninos
- There are potential implications for the predictability of ENSO

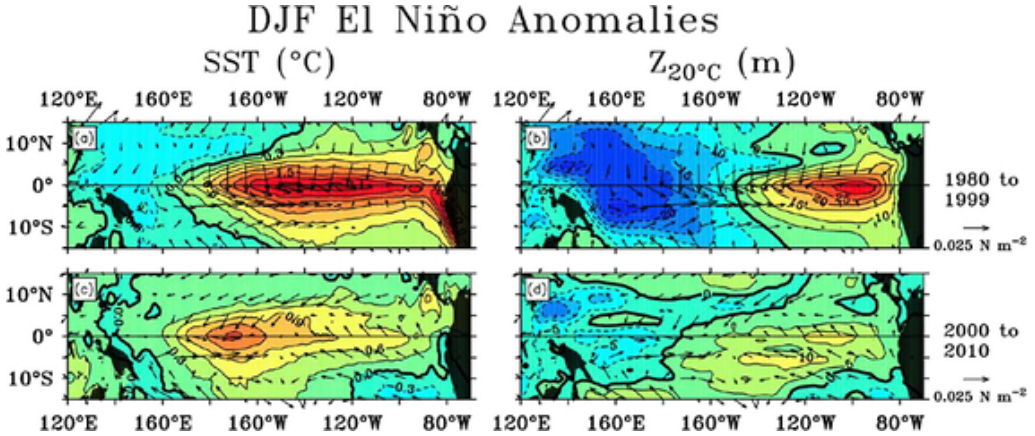

1 of 4

Greenland ice core evidence for spatial and temporal variability of the Atlantic Multidecadal Oscillation

Petr Chylek, Chris Folland, Leela Frankcombe, Henk Dijkstra, Glen Lesins, Manvendra Dubey

First Published: 3 May 2012 Vol: 39, L09705 | DOI: 10.1029/2012GL051241

KEY POINTS

- The past history of the AMO is preserved in ice core data
- The dominant quasi-periodicities are those of 20 years and 45-65 years
- The origin of 20-year periodicity is Atlantic and of 45-65 year the Arctic

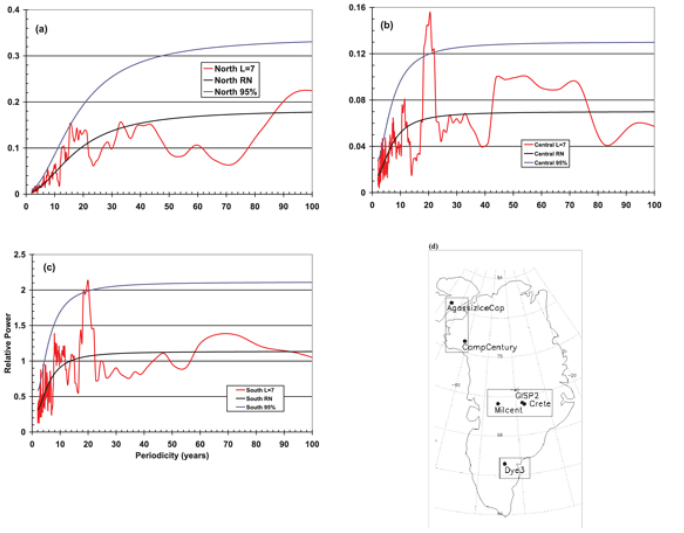

1 of 3

A stochastic method for improving seasonal predictions

L. Batté, M. Déqué

First Published: 4 May 2012 Vol: 39, L09707 | DOI: 10.1029/2012GL051406

KEY POINTS

- Adding stochastic perturbations to CNRM-CM5 improve winter seasonal forecasts
- An optimal perturbation method shows great improvement of correlation scores
- Our method addresses both model systematic errors and lack of spread

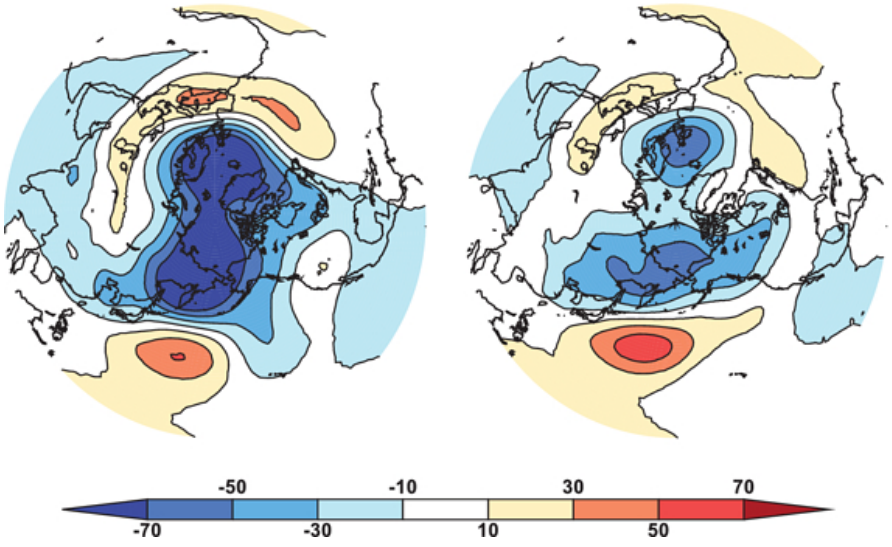

1 of 3

Did we see the 2011 summer heat wave coming?

Lifeng Luo, Yan Zhang

First Published: 5 May 2012 Vol: 39, L09708 | DOI: 10.1029/2012GL051383

KEY POINTS

- Climate extremes like heat wave can be predictable at seasonal time scale
- Operational CFSv2 forecasts consistently predicted the 2011 summer warming
- Forecasts of heat wave became more certain as summer was approaching

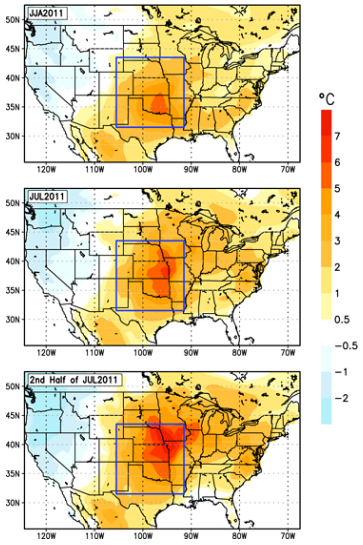

1 of 4

The thermal threshold of the Atlantic meridional overturning circulation and its control by wind stress forcing during glacial climate

A. Oka, H. Hasumi, A. Abe-Ouchi

First Published: 8 May 2012 Vol: 39, L09709 | DOI: 10.1029/2012GL051421

KEY POINTS

- The existence of thermal threshold of AMOC is identified in this study
- The wind stress plays a critical role in controlling thermal threshold value
- Thermal threshold explains different glacial responses of AMOC among models

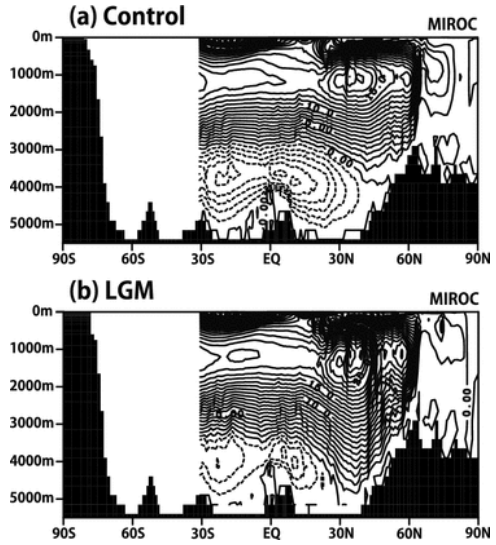

1 of 4

Little Ice Age cold interval in West Antarctica: Evidence from borehole temperature at the West Antarctic Ice Sheet (WAIS) Divide

Anais J. Orsi, Bruce D. Cornuelle, Jeffrey P. Severinghaus

First Published: 9 May 2012 Vol: 39, L09710 | DOI: 10.1029/2012GL051260

KEY POINTS

- Cold interval from 1300 to 1800 C.E. at WAIS Divide
- The 1400-1800 C.E. was 0.52+/-0.28 deg C colder than the last 100 years
- Cooling broadly synchronous to Greenland cooling, with lesser amplitude

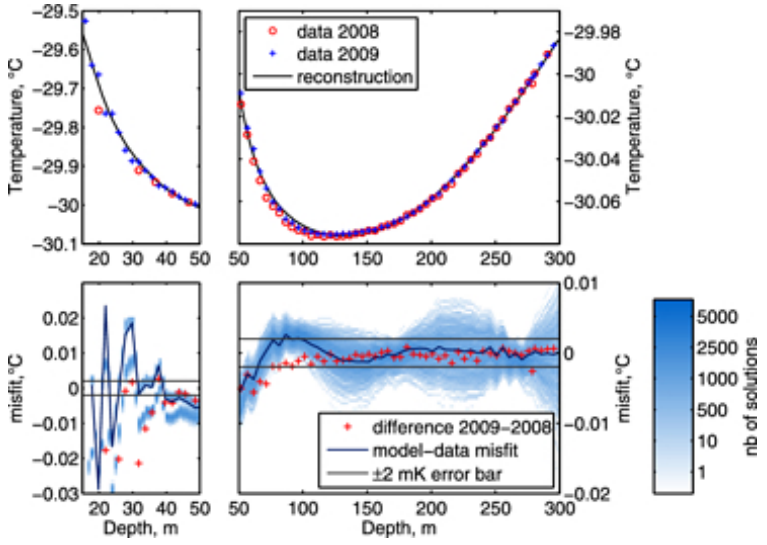

1 of 5

Moisture flux convergence in regional and global climate models: Implications for droughts in the southwestern United States under climate change

Yanhong Gao, L. Ruby Leung, Eric P. Salathé Jr., Francina Dominguez, Bart Nijssen, Dennis P. Lettenmaier

First Published: 10 May 2012 Vol: 39, L09711 | DOI: 10.1029/2012GL051560

KEY POINTS

- Net precipitation projections for the southwestern US differ
- RCMs better resolve transient eddies and their interactions with mountains
- As a result, RCMs show less drying for the southwestern US than paired GCMs

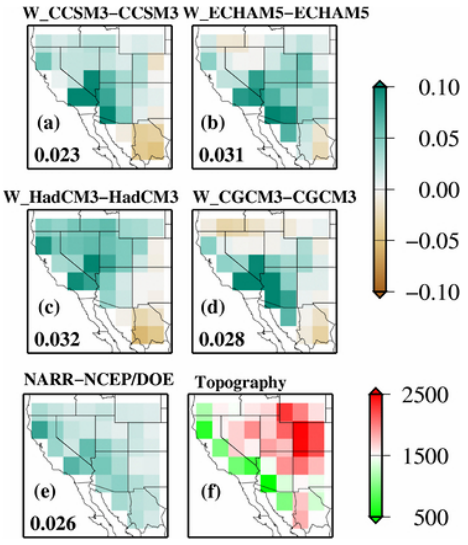

1 of 2

Predicting land cover changes in the Amazon rainforest: An ocean-atmosphere-biosphere problem

Marcos Paulo Santos Pereira, Ana Cláudia Mendes Malhado, Marcos Heil Costa

First Published: 15 May 2012 Vol: 39, L09713 | DOI: 10.1029/2012GL051556

KEY POINTS

- SST variation may decrease ensemble for tropical evergreen rainforest and savanna
- The vegetation types in the Amazon rainforest are linked to the SST

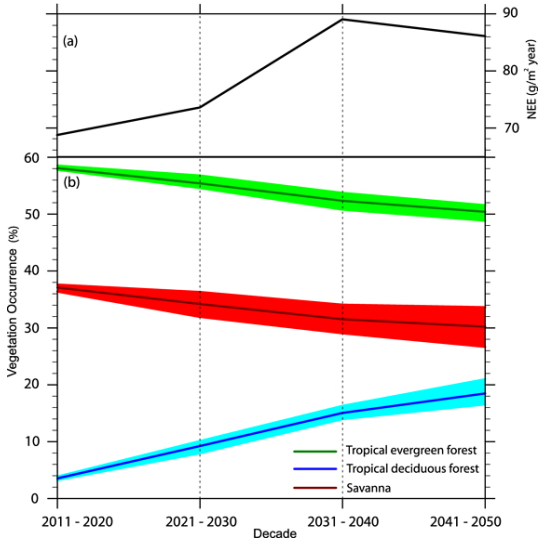

1 of 3

Forcing, feedbacks and climate sensitivity in CMIP5 coupled atmosphere-ocean climate models

Timothy Andrews, Jonathan M. Gregory, Mark J. Webb, Karl E. Taylor

First Published: 15 May 2012 Vol: 39, L09712 | DOI: 10.1029/2012GL051607

KEY POINTS

- Range of eqm climate sensitivity (2.1-4.7K) is similar to that found in CMIP3
- Differences in cloud feedbacks continue to be a large source of this uncertainty
- Some models show small deviations from linear behaviour

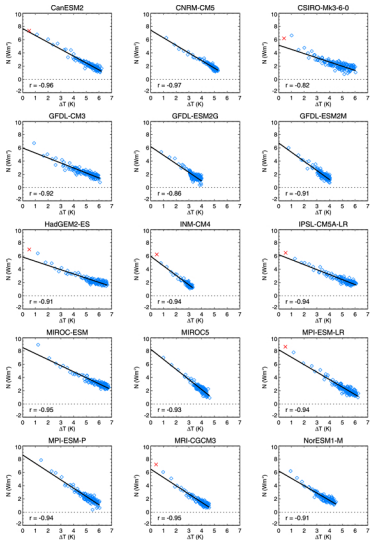

1 of 3

Hydrology and Land Surface Studies

Morphology, propagation dynamics and scaling characteristics of drying fronts in porous media

N. Shokri, Muhammad Sahimi, D. Or

First Published: 2 May 2012 Vol: 39, L09401 | DOI: 10.1029/2012GL051506

KEY POINTS

- Hydrophobicity reduces velocity of DF displacement
- Wettability weakly affects the fractal dimension and roughness exponent of DF
- Lesser wettability limits the extent of film region and the evaporation rate

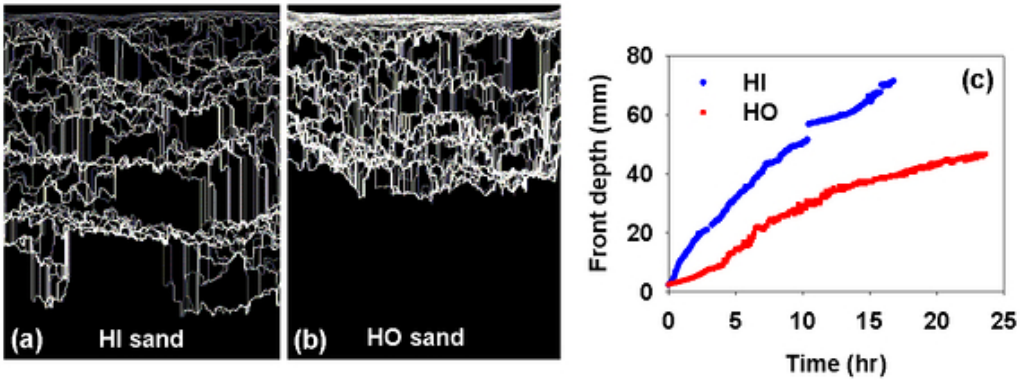

1 of 5

Past and future contribution of global groundwater depletion to sea-level rise

Yoshihide Wada, Ludovicus P. H. van Beek, Frederiek C. Sperna Weiland, Benjamin F. Chao, Yun-Hao Wu, Marc F. P. Bierkens

First Published: 8 May 2012 Vol: 39, L09402 | DOI: 10.1029/2012GL051230

KEY POINTS

- Future projection of the contribution of groundwater depletion to sea-level rise
- The contribution of GW depletion outweighs the negative contribution by dams
- GW depletion will be a dominant contribution to SLR from land in coming decades

Highlight

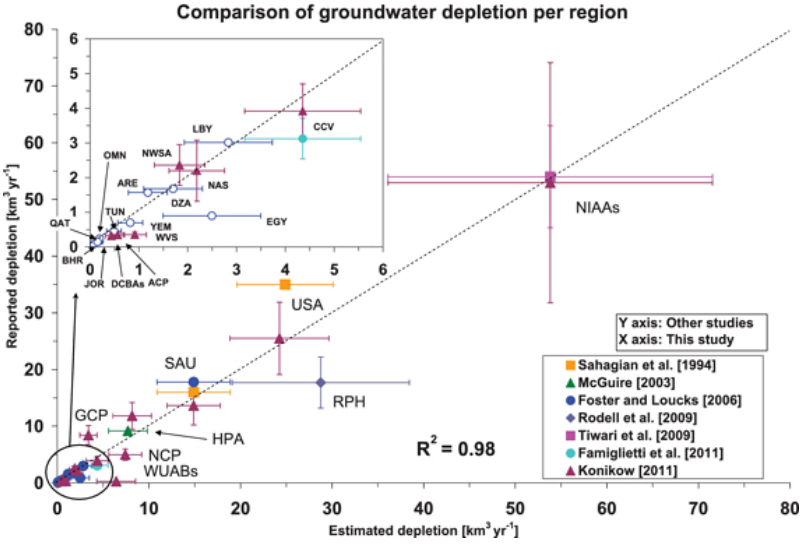

1 of 3

Increasing subsurface water storage in discontinuous permafrost areas of the Lena River basin, Eurasia, detected from GRACE

I. Velicogna, J. Tong, T. Zhang, J. S. Kimball

First Published: 9 May 2012 Vol: 39, L09403 | DOI: 10.1029/2012GL051623

KEY POINTS

- Increase in subsurface water storage in discontinuous permafrost
- Quantitative agreement between GRACE and climatological data
- New methodology to solve for precipitation bias, of interest to climate modelers

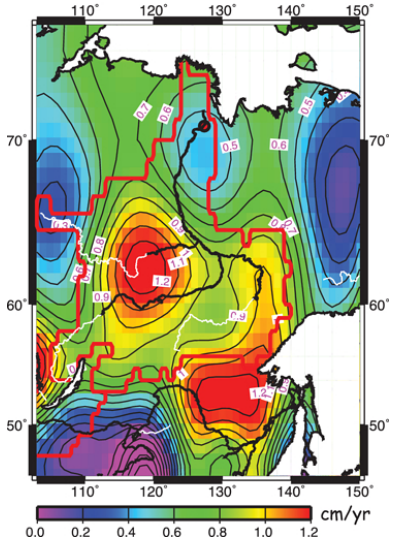

1 of 3

Dynamic dissolution of halite rock during flow of diluted saline solutions

N. Weisbrod, C. Alon-Mordish, E. Konen, Y. Yechieli

First Published: 10 May 2012 Vol: 39, L09404 | DOI: 10.1029/2012GL051306

KEY POINTS

- During flow of unsaturated solutions, dissolution is being developed as channels
- If flow is very slow, reprecipitation can clog the salt rock
- Solution density and salt structure play a major role in the dynamic dissolution

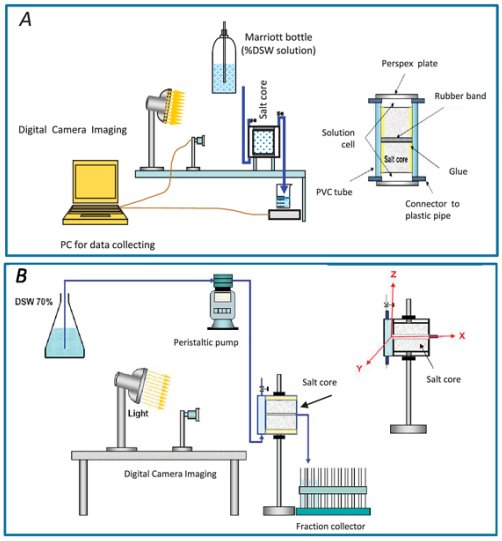

1 of 4

Lake-size dependency of wind shear and convection as controls on gas exchange

Jordan S. Read, David P. Hamilton, Ankur R. Desai, Kevin C. Rose, Sally MacIntyre, John D. Lenters, Robyn L. Smyth, Paul C. Hanson, Jonathan J. Cole, Peter A. Staehr, et al

First Published: 10 May 2012 Vol: 39, L09405 | DOI: 10.1029/2012GL051886

KEY POINTS

- Convection was consistently a larger turbulence source than wind for small lakes
- Convection and wind shear have different diurnal seasonal and geographic pattern
- Wind-only methods for gas exchange are not appropriate for small lakes

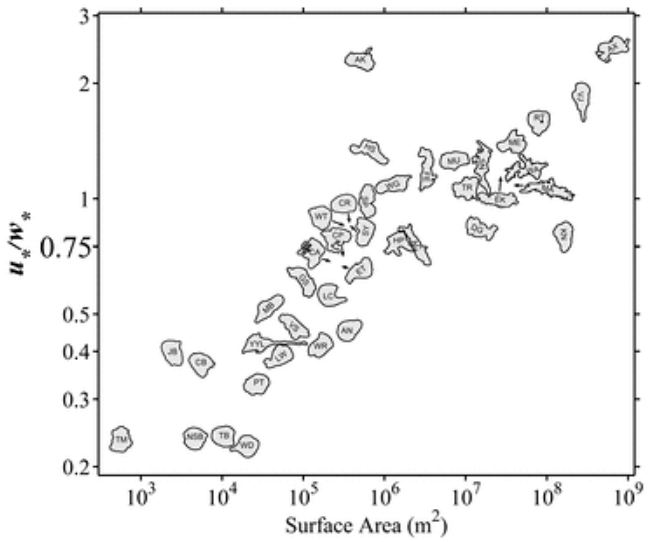

1 of 3

Systematic and random error components in satellite precipitation data sets

Amir AghaKouchak, Ali Mehran, Hamidreza Norouzi, Ali Behrangi

First Published: 11 May 2012 Vol: 39, L09406 | DOI: 10.1029/2012GL051592

KEY POINTS

- Error decomposition of satellite precipitation data
- Characteristics of systematic error in summer and winter data
- Proportionality of systematic error of precipitation to rain rate

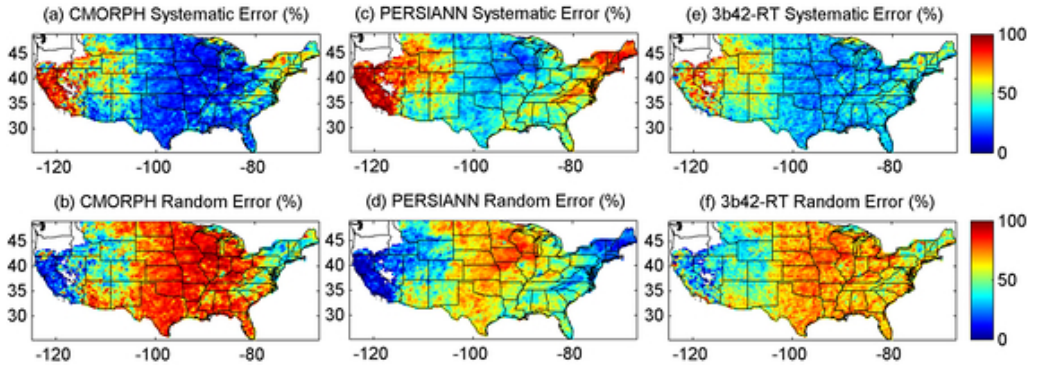

1 of 5

Oceans

Relative role of wind forcing and riverine nutrient input on the extent of hypoxia in the northern Gulf of Mexico

Y. Feng, S. F. DiMarco, G. A. Jackson

First Published: 3 May 2012 Vol: 39, L09601 | DOI: 10.1029/2012GL051192

KEY POINTS

- River discharge plus wind persistence best explains area variability
- The optimal period to consider wind persistence is 32 days
- Bootstrap analysis show that the relationship are robust

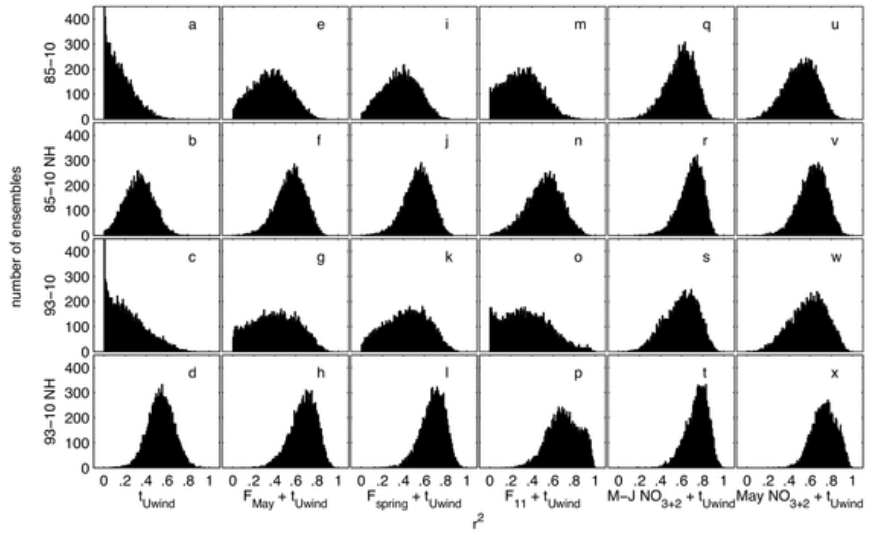

1 of 1

Ensemble ENSO hindcasts initialized from multiple ocean analyses

Jieshun Zhu, Bohua Huang, Lawrence Marx, James L. Kinter III, Magdalena A. Balmaseda, Rong-Hua Zhang, Zeng-Zhen Hu

First Published: 4 May 2012 Vol: 39, L09602 | DOI: 10.1029/2012GL051503

KEY POINTS

- It is a first try to study the sensitivity of ENSO prediction to different ODAs
- There is substantial spread in ENSO prediction skill with different ODAs
- Ensemble prediction by multi-ODAs can provide more reliable ENSO prediction

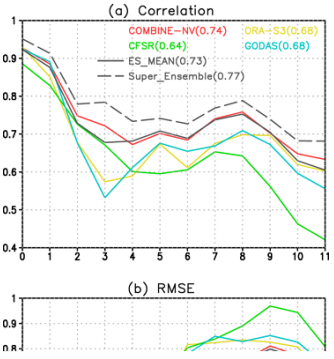

1 of 4

Surges along the Honolulu coast from the 2011 Tohoku tsunami

Yoshiki Yamazaki, Kwok Fai Cheung, Geno Pawlak, Thorne Lay

First Published: 5 May 2012 Vol: 39, L09604 | DOI: 10.1029/2012GL051624

KEY POINTS

- Modeling of 2011 Tohoku tsunami from earthquake rupture to currents in Hawaii
- Validation of nearshore tsunami currents with measurements
- Relation between nearshore currents and periods of tsunami waves

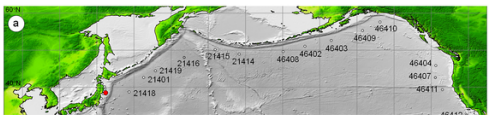

1 of 5

Improving tsunami warning using commercial ships

James H. Foster, Benjamin A. Brooks, Dailin Wang, Glenn S. Carter, Mark A. Merrifield

First Published: 5 May 2012 Vol: 39, L09603 | DOI: 10.1029/2012GL051367

KEY POINTS

- A 10 cm tsunami was detected in the open ocean using ship-borne GPS
- Key tsunami wave parameters can be estimated, even for moderate to small signals
- The commercial shipping fleet could be used to form a tsunami monitoring network

Highlight

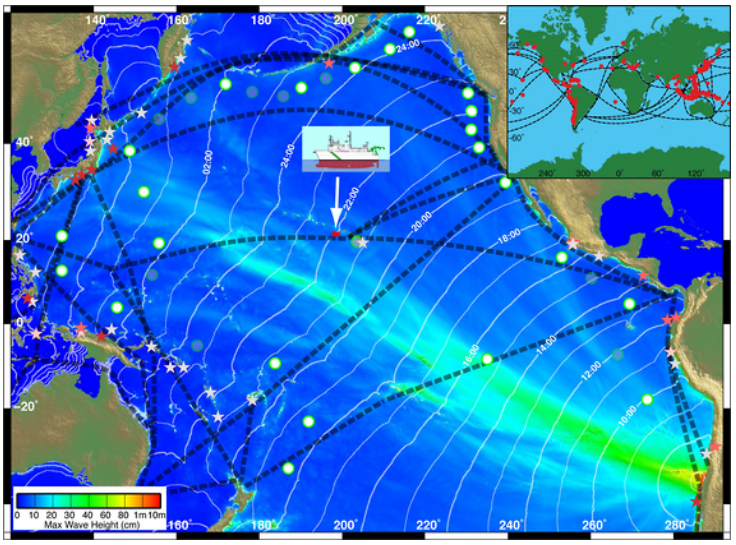

1 of 4

Drivers of the projected changes to the Pacific Ocean equatorial circulation

A. Sen Gupta, A. Ganachaud, S. McGregor, J. N. Brown, L. Muir

First Published: 11 May 2012 Vol: 39, L09605 | DOI: 10.1029/2012GL051447

KEY POINTS

- New Guinea Undercurrent and Equatorial Undercurrent projected to intensify
- Intensification driven by wind stress curl changes in the Southern Hemisphere
- Shallow water model demonstrates role of wind in driving projected changes

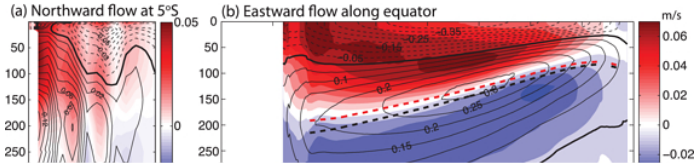

1 of 4

Response of the Atlantic Ocean circulation to Greenland Ice Sheet melting in a strongly-eddying ocean model

W. Weijer, M. E. Maltrud, M. W. Hecht, H. A. Dijkstra, M. A. Kliphuis

First Published: 11 May 2012 Vol: 39, L09606 | DOI: 10.1029/2012GL051611

KEY POINTS

- Mesoscale features impact the response of the AMOC to GrIS meltwater input
- Overall AMOC decline on decadal time scales robust
- Transient response is more gradual and more persistent when resolving eddies

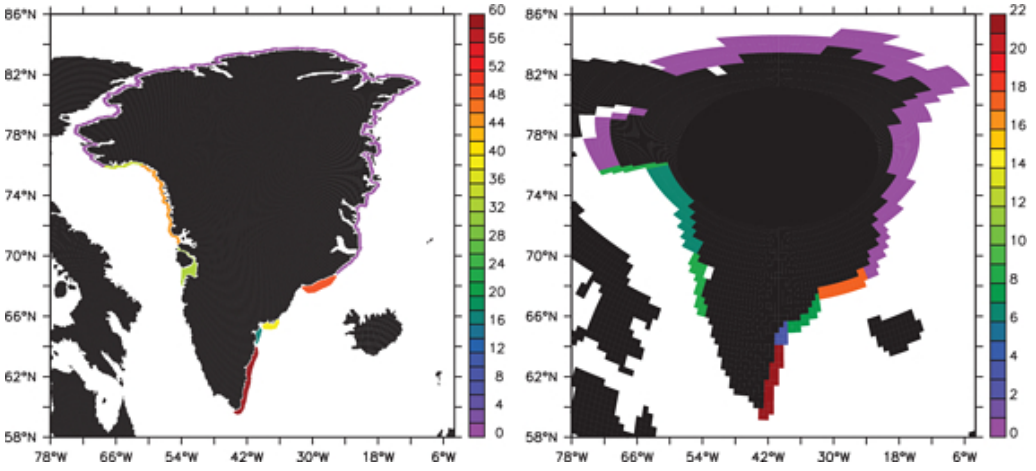

1 of 3

Planets

Seasonally active slipface avalanches in the north polar sand sea of Mars: Evidence for a wind-related origin

Briony H. N. Horgan, James F. Bell III

First Published: 10 May 2012 Vol: 39, L09201 | DOI: 10.1029/2012GL051329

KEY POINTS

- Alcoves on Martian dune slipfaces form when aeolian deposition causes avalanches
- Alcove formation is not related to spring CO2 sublimation
- Large avalanche size may be due to surface cohesion or induration

Highlight

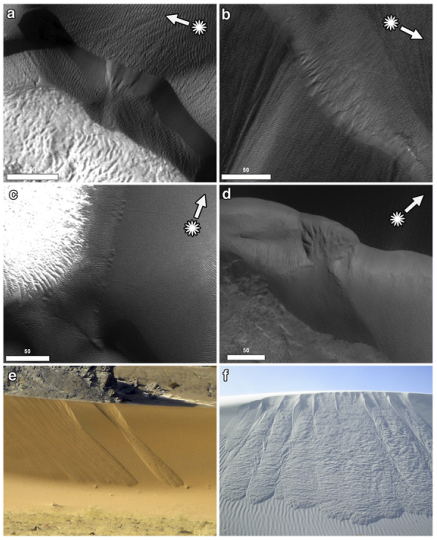

1 of 3

Is Mercury a volatile-rich planet?

Francis M. McCubbin, Miriam A. Riner, Kathleen E. Vander Kaaden, Laura K. Burkemper

First Published: 12 May 2012 Vol: 39, L09202 | DOI: 10.1029/2012GL051711

KEY POINTS

- Mercury's oxygen fugacity is the lowest of the terrestrial planets
- Mercury could be volatile-depleted, which is masked by its low oxygen fugacity
- Experimental data applicable to magmatic systems on Mercury are very limited

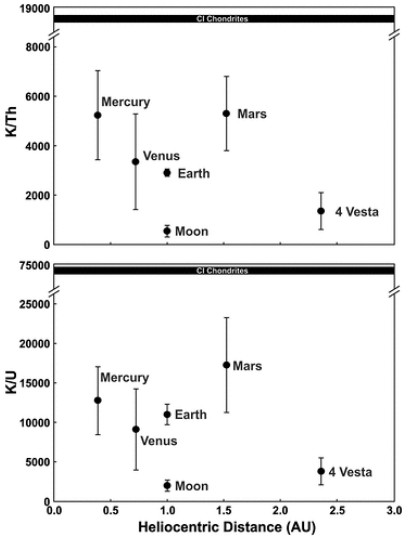

1 of 3

Two-dimensional distribution of volatiles in the lunar regolith from space weathering simulations

Dana M. Hurley, David J. Lawrence, D. Benjamin J. Bussey, Richard R. Vondrak, Richard C. Elphic, G. Randall Gladstone

First Published: 12 May 2012 Vol: 39, L09203 | DOI: 10.1029/2012GL051105

KEY POINTS

- Ice detectable by radar disappears in < 100 Myr
- Widespread surface frost represents continual processes
- A lateral range of 10 m is sufficient to acquire measurements of heterogeneity

Open Access

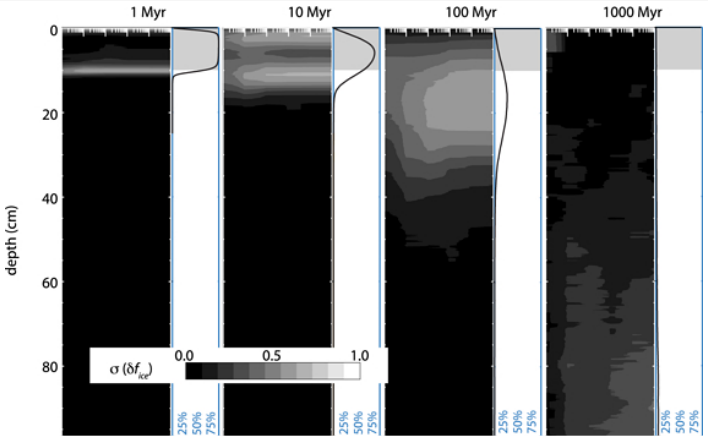

1 of 4

Areas of permanent shadow in Mercury's south polar region ascertained by MESSENGER orbital imaging

Nancy L. Chabot, Carolyn M. Ernst, Brett W. Denevi, John K. Harmon, Scott L. Murchie, David T. Blewett, Sean C. Solomon, Ellen D. Zhong

First Published: 12 May 2012 Vol: 39, L09204 | DOI: 10.1029/2012GL051526

KEY POINTS

- MESSENGER images provide first results for Mercury's south pole
- Mercury's polar radar-bright features map to permanent shadow
- Radar-bright features in shadowed areas are consistent with water ice on Mercury

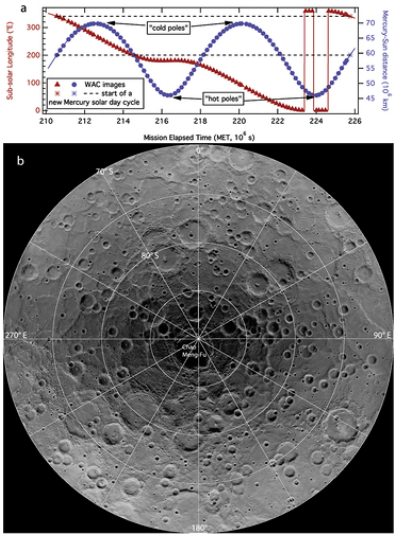

1 of 4

Solid Earth

Generalized joint inversion of multimodal geophysical data using Gramian constraints

Michael S. Zhdanov, Alexander Gribenko, Glenn Wilson

First Published: 1 May 2012 Vol: 39, L09301 | DOI: 10.1029/2012GL051233

KEY POINTS

- Introduction of gramian constraints as regularization
- Simultaneous joint inversion of multi-modal geophysical data
- Ability to discriminate mineralogy from joint inversion of potential field data

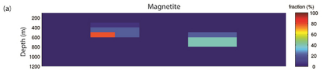

1 of 3

Q_P and Q_S in the upper mantle beneath the Iberian peninsula from recordings of

the very deep Granada earthquake of April 11, 2010

F. Mancilla, E. Del Pezzo, D. Stich, J. Morales, J. Ibañez, F. Bianco

First Published: 2 May 2012 Vol: 39, L09303 | DOI: 10.1029/2012GL050947

KEY POINTS

- A rare, very deep earthquakes probes the upper-mantle beneath Iberia
- Upper mantle attenuation is high between 0.25 Hz and 8 Hz
- Scattering is the dominant mechanism, indicating strong heterogeneity

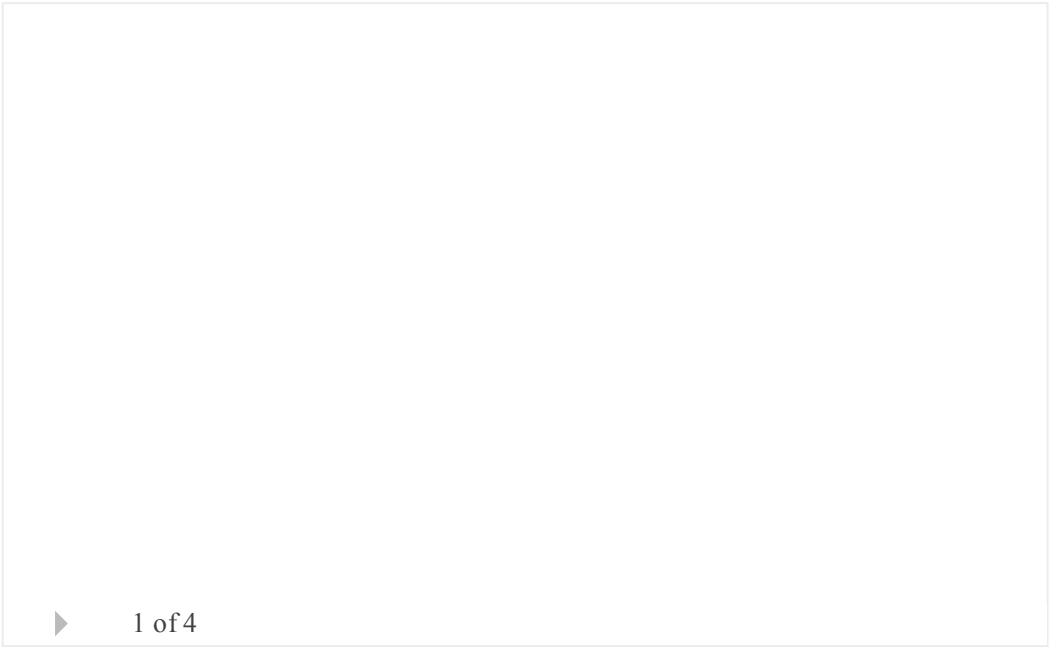

Influence of pore-pressure on the event-size distribution of induced earthquakes

C. E. Bachmann, S. Wiemer, B. P. Goertz-Allmann, J. Woessner

First Published: 2 May 2012 Vol: 39, L09302 | DOI: 10.1029/2012GL051480

KEY POINTS

- The b-values of induced earthquakes decrease with distance from the injection point
- We propose a pressure-driven geomechanical model to explain our observation
- We estimate the probability of induced large magnitude events in space and time

1 of 5

Spatial variations in earthquake source characteristics within the 2011 Mw = 9.0 Tohoku, Japan rupture zone

Susan L. Bilek, Heather R. DeShon, E. Robert Engdahl

First Published: 3 May 2012 Vol: 39, L09304 | DOI: 10.1029/2012GL051399

KEY POINTS

- Spatial variations exist for relocated earthquakes in the 2011 Tohoku area
- Long duration events do not lie within 2011 high slip zone
- Long duration events do occur within region of 1896 tsunami earthquake

1 of 4

Real-time inversion of GPS data for finite fault modeling and rapid hazard assessment

Brendan W. Crowell, Yehuda Bock, Diego Melgar

First Published: 5 May 2012 Vol: 39, L09305 | DOI: 10.1029/2012GL051318

KEY POINTS

- Real-time GPS can be used for rapid source modeling
- Rapid source modeling with GPS takes 2 minutes to reach a stable solution
- Integration of GPS into early warning and rapid response is critical

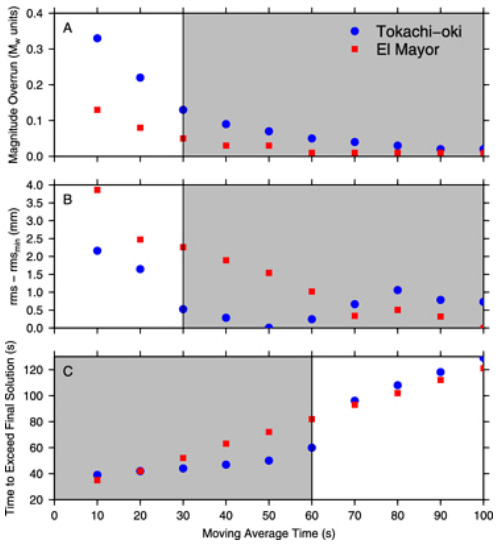

1 of 3

Unusual shallow normal-faulting earthquake sequence in compressional northeast Japan activated after the 2011 off the Pacific coast of Tohoku earthquake

Kazutoshi Imanishi, Ryosuke Ando, Yasuto Kuwahara

First Published: 5 May 2012 Vol: 39, L09306 | DOI: 10.1029/2012GL051491

KEY POINTS

- Finding of a locally formed extensional stress regime at northeast Japan
- Pre-shock extensional stress regime is needed to trigger the normal-faulting EQs
- Implication for the occurrence of past repeated megathrust EQs

1 of 4

Farallon slab detachment and deformation of the Magdalena Shelf, southern Baja California

Daniel Brothers, Alistair Harding, Antonio González-Fernández, W. Steven Holbrook, Graham Kent, Neal Driscoll, John Fletcher, Dan Lizarralde, Paul Umhoefer, Gary Axen

First Published: 8 May 2012 Vol: 39, L09307 | DOI: 10.1029/2011GL050828

KEY POINTS

- First detailed crustal image of southern Baja California microplate
- Beneath the western Baja California margin, ~40 km of relic Farallon slab exists
- Relationship between slab detachment, uplift, magmatism, and transtension

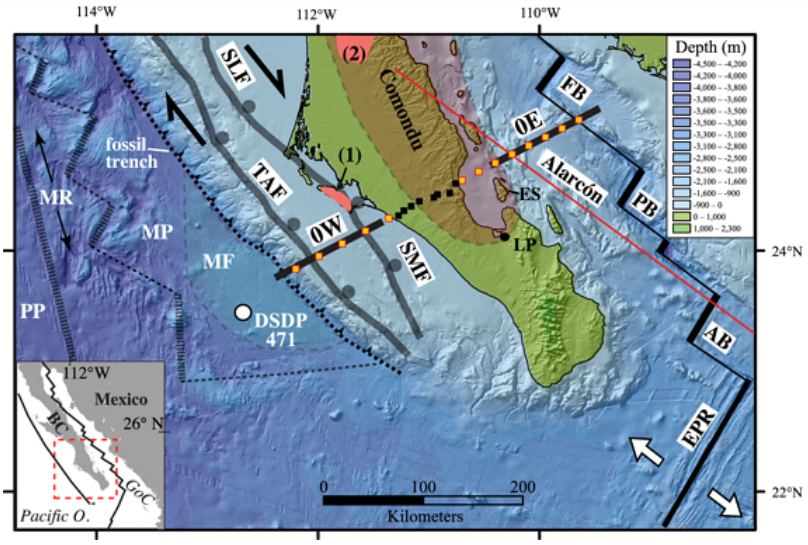

1 of 4

Localized seismic anisotropy associated with long-term slow-slip events beneath southern Mexico

Teh-Ru Alex Song, YoungHee Kim

First Published: 9 May 2012 Vol: 39, L09308 | DOI: 10.1029/2012GL051324

KEY POINTS

- Use seismic anisotropy to probe structural control on slow slip events
- Llong-term slow slip associated with weak clay minerals and high fluid pressure
- Semi-ductile shear zone may display composite slip behavior

1 of 4

Monitoring seismic velocity change caused by the 2011 Tohoku-oki earthquake using ambient noise records

Shohei Minato, Takeshi Tsuji, Shiro Ohmi, Toshifumi Matsuoka

First Published: 12 May 2012 Vol: 39, L09309 | DOI: 10.1029/2012GL051405

KEY POINTS

- Ambient noise data shows the crustal velocity change in Tohoku-oki earthquake
- Velocity change is clearly observed at mainshock and aftershocks
- The velocity change is explained by both strain change and surface damage

1 of 4

Temporal change in shear velocity and polarization anisotropy related to the 2011 M9.0 Tohoku-Oki earthquake examined using KiK-net vertical array data

Ryota Takagi, Tomomi Okada

First Published: 15 May 2012 Vol: 39, L09310 | DOI: 10.1029/2012GL051342

KEY POINTS

- Temporal change in shear velocity and polarization anisotropy were observed
- Anisotropy change is smaller than velocity change
- Static stress change is not sufficient to change fast direction of shear wave

1 of 5

Lithospheric flexure in the Sichuan Basin and Longmen Shan at the eastern edge of Tibet

Eric J. Fielding, Dan McKenzie

First Published: 15 May 2012 Vol: 39, L09311 | DOI: 10.1029/2012GL051680

KEY POINTS

- Flexure of Sichuan lithosphere supports Longmen Shan at eastern edge of Tibet
- Eastern Tibet has low elastic thickness, Sichuan Basin greater thickness
- New GOCE satellite gravity improves flexure estimates

1 of 3

Space Sciences

Radial distributions of equatorial phase space density for outer radiation belt electrons

D. L. Turner, V. Angelopoulos, Y. Shprits, A. Kellerman, P. Cruce, D. Larson

First Published: 11 May 2012 Vol: 39, L09101 | DOI: 10.1029/2012GL051722

KEY POINTS

- Error and uncertainty in PSD for fixed invariants can and should be quantified
- PSD distributions for outer belt electrons are most often energy dependent
- Relativistic PSD distributions are typically peaked at around L*=5.5

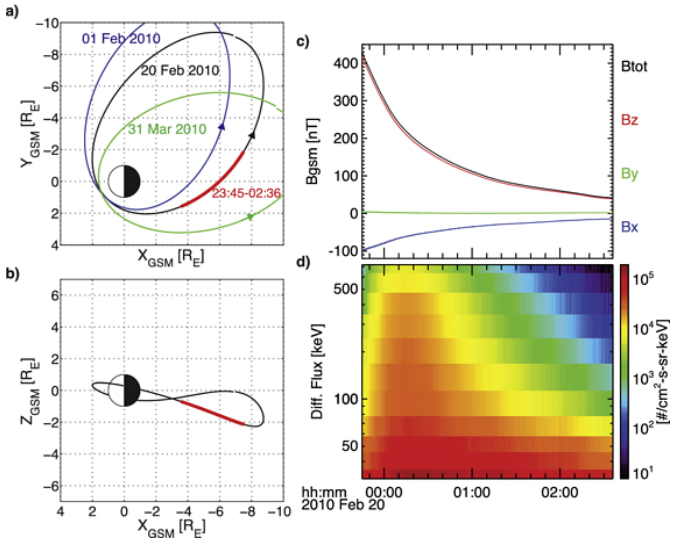

1 of 4

Current Issue

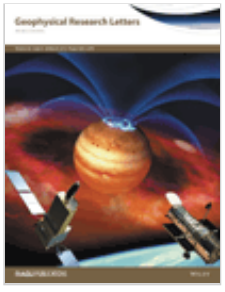

Volume 42
Issue 6
28 March 2015

All Issues
Browse a free sample issue

Find an article

and

or

Stay Connected to Eos

Journal Resources

Call for Papers

Special Section Proposal Form

Personal Choice

Terms of Use

Cover Gallery

Institutional Subscription Rates

Get RSS Feed

Featured Special Collection

The Early Results from the Van Allen Probes

NASA's Van Allen Probes mission is designed to acquire data to solve key questions

about the energetics and dynamics of the Earth's Van Allen Radiation belts that have arisen from active research in the domain in the past decades.

Editors' Highlights

- **What Causes Sunspot Pairs?**
- **Water Beneath the Surface of Mars, Bound up in Sulfates**
- **When Predicting Drought Risk, Do Not Overlook Temperature**
- **Changing Patterns in U.S. Air Quality**

See all »

Download the app

Download the Geophysical Research Letters app on your iPad

Upcoming AGU Meetings

Triennial Earth-Sun Summit

26 Apr - 1 May 2015
Indianapolis, Indiana, USA

2015 Joint Assembly

3-7 May 2015
Montreal, Canada

Chapman Conference on Evolution of the Asian Monsoon and its Impact on Landscape, Environment and Society: Using the Past as the Key to the Future

14-19 June 2015
Hong Kong SAR, China

See all »